

Neutral Beam Driven Global Alfvén Eigenmodes in the Wendelstein W7-AS Stellarator

A. Weller,¹ D. A. Spong,² R. Jaenicke,¹ A. Lazaros,¹ F. P. Penningsfeld,¹ S. Sattler,¹ W7-AS Team,¹ and NBI Group¹

¹Max-Planck-Institut für Plasmaphysik, IPP-EURATOM-Association, D-85740 Garching, Germany

²Oak Ridge National Laboratory, Oak Ridge, Tennessee 37831

(Received 1 June 1993; revised manuscript received 12 November 1993)

During neutral beam injection coherent magnetohydrodynamic activity occurs at low and medium β , which is driven by the energetic beam particles. An interpretation is given in terms of marginally stable global Alfvén eigenmodes (GAE), which are destabilized by Landau resonances of the fast circulating particles. Toroidicity induced gaps for toroidal Alfvén eigenmodes do not occur in W7-AS, but GAE modes in gaps below the shear Alfvén continua can be excited. This is investigated within a gyrofluid model, which has been used successfully for tokamak cases previously.

PACS numbers: 52.55.Hc

Introduction.—The effect of the destabilization of discrete magnetohydrodynamic (MHD) modes in the shear Alfvén spectrum by energetic particles has received increasing attention over the last years from experiment and theory. The confinement of fusion α particles and energetic particles used for plasma heating and for current drive is an important issue in future fusion devices. Wave particle resonances are predicted to cause enhanced losses of fast particles [1,2]. Therefore, these instabilities could impose additional operating constraints in the reactor regime.

Global Alfvén waves have been identified experimentally in large tokamak devices as toroidal Alfvén eigenmodes (TAE) [3–6], which are excited inside toroidicity induced gaps of the shear Alfvén continua. Considerable progress has been made in achieving a good quantitative description by theoretical models [7–12].

Modification of the Alfvén spectra and the particle destabilization mechanisms are expected in stellarators, where the magnetic field is nonaxisymmetric and the magnetic shear and the aspect ratio are different from tokamaks. If the helical magnetic field ripple is large, helicity induced discrete Alfvén modes [13] can be formed. In the partially optimized stellarator Wendelstein W7-AS [14] ($R=2$ m, $a\leq 0.17$ m, 5 field periods, modular stellarator coil system, additional toroidal field coils), the most relevant effects of the magnetic configuration are associated with the weak shear, by which low order rational values of the rotational transform $\iota=1/q$ can be avoided. The stability of resonant pressure driven modes relies mainly on a magnetic well, which is in the order of 2%. Optimum confinement in W7-AS is found in the vicinity of $\iota=1/3$ and $1/2$ due to the lower density of low order rational values $\iota=n/m$. Therefore, couplings between adjacent poloidal mode numbers m and $m+1$ (with same toroidal mode number n) and consequently toroidicity induced gaps cannot occur. However, gaps below the minima of the low order shear Alfvén continua with $(m,n)=(2,1)$, $(3,1)$, $(5,2)$, and $(5,3)$ are typically formed. Discrete global Alfvén eigenmodes (GAE) with frequencies $\omega_{\text{GAE}}\leq k_{\parallel}v_A\equiv\omega_A$ [parallel wave num-

ber $k_{\parallel}=(m\iota-n)/R$, Alfvén speed $v_A=B/\sqrt{4\pi n_i m_i}$, shear Alfvén continuum frequency ω_A] are predicted in the Alfvén spectrum [15–17].

In tokamaks GAE modes with $n/m\iota>0$ (same helicity as for main field) have not been observed. This can be due to the requirement of weak central shear and $\iota<1$ (in order to keep the gap open). In the case where $k_{\parallel}=0$, GAE modes do not exist, and kink modes may occur [18,19]. GAE modes with $n/m\iota<0$ have been predicted and seen as resonances in radio frequency excitation experiments [15,20–22]. Energetic particle destabilization in the latter case has not been observed because of the high excitation energies required (large k_{\parallel} and frequencies). In the case of W7-AS a weak shear with $\iota<1$ and the absence of kink modes (no toroidal current) allow destabilization of $n/m\iota>0$ GAE modes. Since this type of GAE mode has been observed the first time in experiment, the present results, therefore, are believed to be relevant with respect to the performance of present and future stellarators like the proposed W7-X device. They also contribute to a wider theoretical understanding of the Alfvén spectra in toroidal devices by combining the results of stellarators with those of tokamaks.

Neutral beam driven mode activity and relation to global Alfvén waves.—Plasmas in Wendelstein W7-AS are produced and heated by electron cyclotron resonance heating (ECRH) at main fields of 1.25 or 2.5 T ($P_{\text{ECRH}}<0.8$ MW, 70 GHz). Neutral beam injection (NBI) with two almost tangential beam lines (codirection and counterdirection, $P_{\text{NBI}}<1.6$ MW, 45 keV hydrogen beam) gives access to higher densities and higher plasma pressure.

During NBI coherent mode activity with frequencies in the range 20–35 kHz is detected. The modes are clearly driven by circulating energetic particles, since they decay rapidly after NBI switch off on a time scale of ≈ 0.3 ms, which is significantly shorter compared with typical slowing down times of ≈ 5 ms and energy confinement times of ≈ 10 ms (Fig. 1). Mode numbers (m,n) and the direction of propagation are derived from x-ray and Mirnov data. The mode spectrum is dominated by single

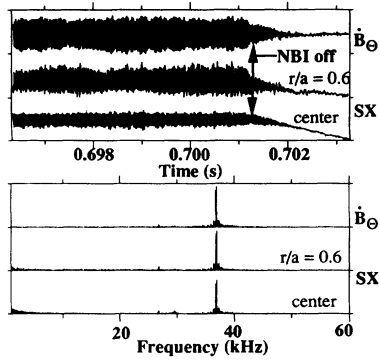


FIG. 1. Coherent modes with sharp frequency lines are driven by NBI. They decay rapidly after NBI switch off (signals from Mirnov coil and soft x-ray diodes).

small (positive) numbers $(m,n) = (3,1)$, $(5,2)$, $(2,1)$, and $(5,3)$ depending on the χ profile and the proximity to prominent rational values. The mode helicity is close to that of the equilibrium field ($n/m\chi > 0$, very small k_{\parallel}) as inferred from phase analysis at different toroidal positions. This is in contrast with calculations and observations in tokamaks and could be explained by the different MHD mode spectrum in stellarators due to the absence of the global toroidal current.

The mode propagation does not depend on the direction of beam injection (co/counter), but changes with the direction of the magnetic field. In each case the instability was found to propagate in the ion diamagnetic drift direction (thermal and fast ions), opposite to the case of pressure driven MHD activity at lower frequencies. The frequencies scale with the Alfvén velocity and agree with predictions for GAE's. The result of a magnetic field scan using nonresonantly produced target plasma [23] for NBI is shown in Fig. 2. The frequencies cannot be explained by fluid drifts or plasma rotation. Kinetic ballooning modes [24] can be excluded because the plasma pressure is far below the ideal ballooning stability threshold and the frequencies should scale differently ($\approx \omega_{*i}$). Therefore, the modes are attributed to Alfvén waves.

Destabilization occurs at intermediate densities ($\langle n_e \rangle \leq 1 \times 10^{20} \text{ m}^{-3}$) and in the lower β range [$\beta_e \approx (1-4) \times 10^{-3}$, $\beta_b \approx (2-6) \times 10^{-4}$ with β_e , β_b the electron and fast ion beta], where $T_e \approx T_i \leq 400 \text{ eV}$. Under these conditions the full energy hydrogen injection velocity v_b marginally reaches the Alfvén velocity v_A at low field (1.25 T), but typically one finds $v_b/v_A = 0.35-1.0$.

The radial mode structure is centered around $r/a = 0.4-0.7$ in the pressure gradient region, and its extent is up to about $1/2$ of the plasma radius as deduced from x rays (Fig. 3) and electron cyclotron emission (ECE). Even the H_α emission is modulated. From the ECE profile measurements the radial displacement function can be derived, which is usually qualitatively consistent with predictions for the fundamental radial eigenfunction. Frequently also weaker satellite lines are found in the

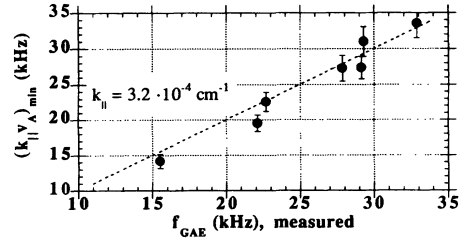


FIG. 2. Scaling of the $(3,1)$ mode frequency in a magnetic field scan (0.9–2.5 T) with the Alfvén velocity. Experimental values are plotted versus the calculated shear Alfvén continuum threshold frequency. The data are fitted with $k_{\parallel} = 3.2 \times 10^{-4} \text{ cm}^{-1}$ at the mode position in consistency with the χ profile [edge value $\chi(a) = 0.35$].

spectrum, which are shifted by up to 30%. In those cases, typically a radial node in the radial eigenfunction is observed.

For a number of different cases the cylindrical shear Alfvén continua $\omega_A = k_{\parallel} v_A$ have been calculated in order to relate the observed frequencies to the upper gap frequencies. An example with reference to the case of the $m/n = 3/1$ mode shown in the previous figures is given in Fig. 4. Experimentally deduced profiles of plasma density and rotational transform have been used to calculate $v_A(r)$ and $k_{\parallel}(r)$. With the observed GAE frequency and injected beam velocity, one can infer over what radial regions particle-wave resonances should occur. The GAE is mainly destabilized by the two sideband resonances $v_b \approx \omega_{\text{GAE}}/k_{\parallel, m \pm 1}$, which enter in as a result of the poloidal variation of the fast ion magnetic drift velocity. For a fixed v_b , ω_{GAE} , n , and m resonances at $\chi_{\text{res}} = n/(m+l) + \Delta\chi$ [where $\Delta\chi = (R/v_b)\omega_{\text{GAE}}/(m+l)$ and $l = 0, \pm 1$] can occur at least one of which presumably must be contained in the χ profile. This is not a significant constraint for a high shear system, but in W7-AS it can crucially determine whether the GAE will be excited and with which part of the fast ion distribution it will resonate. There will also be a shift between co-injected and counterinjected ions, since their drift orbits are displaced in opposite radial directions, leading accordingly to changes in χ_{res} . Taking such effects into account results in the horizontal bars shown in Fig. 3. These mark the radial ranges for the GAE frequencies at which beam wave resonances can take place with velocities down to $1/3$ of the full energy injection speed [$v_b = (1-3) \times 10^8 \text{ cm/s}$].

In this way the observed mode numbers and frequencies could be consistently correlated with predictions for GAE's and on the basis of the cylindrical Alfvén continua. Particular interesting cases are those where GAE's and low frequency ($\leq 8 \text{ kHz}$) pressure driven modes are excited at the same time. The latter do not suffer a rapid decay after NBI switch off, rotate in opposite direction (electron diamagnetic drift), and their poloidal mode number and radial position always differ from that of the

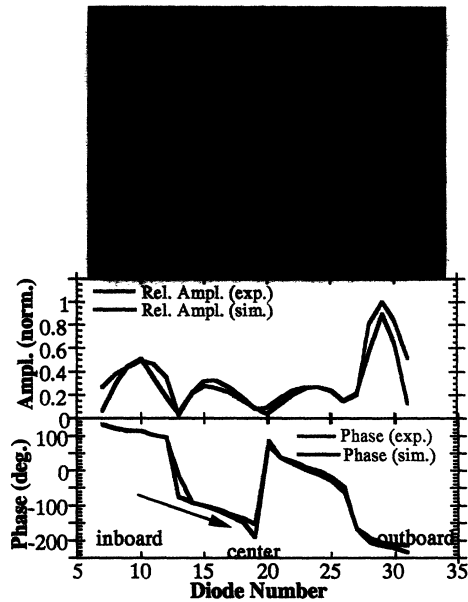


FIG. 3. The poloidal and radial mode structure ($m=3$ in this case) and the direction of propagation is determined from fitting the amplitudes and phases of the x-ray modulation by simulation calculations. On top the radial displacement distribution used in the simulation is given (-2.5 – $+2.5$ cm).

GAE. This behavior can be explained by a rational surface $r=n/m$ inside the plasma, where the pressure driven mode develops, but the GAE of the same mode number cannot exist, because no gap is formed for this particular shear Alfvén continuum ($k_{\parallel}=0$).

An approximate prediction of the stability was obtained from the analytic expression for the linear growth rate of GAE's [16,17]:

$$\frac{\gamma}{\omega_{GAE}} = \frac{\beta_b}{4k_{\parallel}^2 R^2} \left(\frac{\omega_{*b}}{\omega_{GAE}} - 1 \right) (R_{b+} + R_{b-}) - \frac{\beta_e}{4k_{\parallel}^2 R^2} (R_{e+} + R_{e-}). \quad (1)$$

All the terms in this relation originate from the interaction of the wave with the magnetic curvature drift motion of passing particles [$R_{s\pm}(x_{s\pm}) \approx x_{s\pm}$ in W7-AS with $x_{s\pm} \equiv \omega_{GAE}/|k_{\parallel m \pm 1}|v_s$ is proportional to the fraction of resonating ions]. In particular the fast ion drive by inverse Landau damping is associated with its pressure gradient, which is expressed in terms of the diamagnetic drift velocity ω_{*b} . In accordance with the observations, therefore, the drive is only acting on waves propagating in the direction of ω_{*b} . The stabilizing Landau damping terms are due to the gradients in velocity space of fast ions and electrons. For typical cases in W7-AS where $\omega_{*b}/\omega_{GAE}=3$ – 20 , $v_b/v_A=0.35$ – 1.0 , and $\beta_b/\beta_e=0.05$ – 0.15 positive growth rates are obtained from Eq. (1). The excitation as well as the damping are likely to be un-

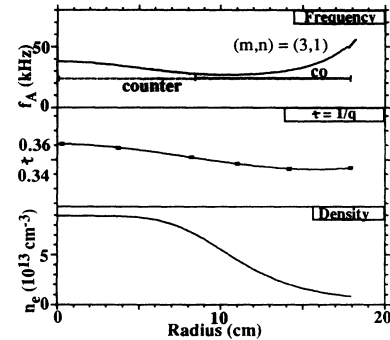


FIG. 4. Shear Alfvén continuum for mode numbers $(m,n)=(3,1)$ (top) obtained with density and r profiles (below) derive from experiment ($B=2.5$ T, $T_e \approx T_i \approx 300$ eV). For the $m=3$ GAE mode an eigenfrequency around 25 kHz is predicted below the continuum as indicated by the horizontal bars, which also mark the radial range of the wave particle resonance (solid line for codirection, dashed line for counterinjection).

derestimated because of the assumed form of the velocity distribution and the neglect of collisional damping [25]. In particular, charge exchange losses of fast ions can modify the slowing down distribution (as indicated by both calculated and measured distributions) in such a way as to decrease the fast ion velocity space damping relative to the configuration space gradient drive, provid-

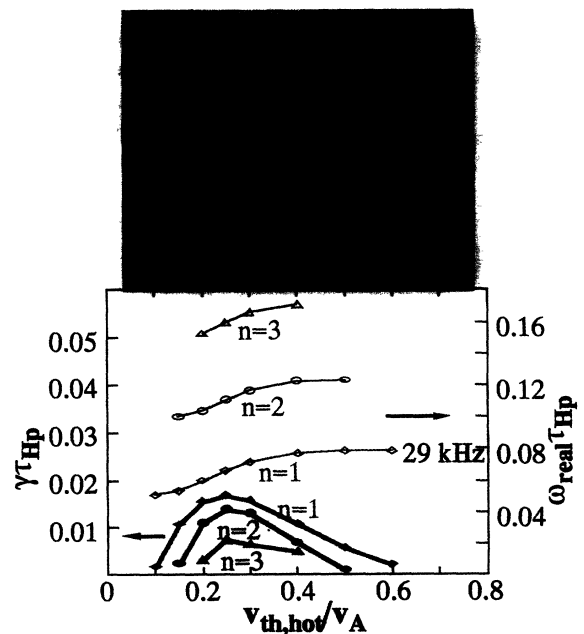


FIG. 5. $(m,n)=3,1$ mode structure from linear gyrofluid model calculation (top). Linear growth rates (including continuum and Landau damping) are highest for $n=1$ and peak around $v_b/v_A(0)=0.2$ – 0.3 . Under the influence of the energetic particles the eigenfrequencies are shifted up (poloidal Alfvén time τ_{Hp}).

ing additional free energy for destabilization. Also, since $v_e/\omega_{\text{GAE}} \cong 1$, collisional dissipation can be important. These two effects, together with density profile changes, could explain why the destabilization preferentially occurs under the conditions of low β and temperature. Towards higher β (typically higher density in W7-AS) β_b/β_e decreases, density profiles flatten, and the shear and collisional damping increase, eventually causing the modes to disappear.

Numerical gyrofluid model calculations—We have analyzed the GAE modes for a few cases with a gyrofluid model with Landau closure for the energetic particles [26]. This approach allows one to include Landau damping/growth effects as well as continuum damping within a fluid description (with reduced MHD) for the background plasma and has been successfully used to describe the behavior of TAE's in DIII-D and TFTR [27].

A simplified large aspect ratio, averaged equilibrium which incorporates magnetic well effects and zero toroidal current is used here. The nonaxisymmetric configuration and noncircular magnetic surfaces in W7-AS are currently neglected. Another simplification used in the gyrofluid equations is that of a Maxwellian fast ion distribution; we match its mean energy to that of a beam slowing down distribution. Further, effects due to finite fast ion orbit width have been omitted. Both linear and nonlinear calculations confirm that the GAE is the fastest growing mode. In the case discussed earlier of the $m/n=3/1$ mode with an ι profile ranging from 0.36 (center) to 0.34 (edge), the calculations (Fig. 5) are in very good agreement with the (i) low beam drive threshold due to weak damping with $\beta_b = 2 \times 10^{-4}$, where electron Landau damping is the most important damping mechanism; (ii) resonant excitation peaking well below $v_b/v_A=1$ as a consequence of low GAE frequency and sideband excitation, where $k_{\parallel, m \pm 1} \gg k_{\parallel, m}$; (iii) very peaked frequency spectrum around 35 kHz; (iv) global radial mode structure; (v) very peaked poloidal mode spectrum; and (vi) nonlinear saturated perturbed magnetic field at the edge $\delta \vec{B}_\theta/B = (1-2) \times 10^{-4}$. Plasma resistivity, which has been incorporated in the model, leads to a suppression of the higher toroidal mode numbers, but does not qualitatively change the dominant $n=1$ component. The results, therefore, remain consistent with experiment.

In conclusion, low frequency GAE modes with small k_{\parallel} are the favored global modes in the shear Alfvén spectrum of low shear devices. They are weakly damped and therefore susceptible to energetic particle destabilization as experimentally observed in the W7-AS stellarator in agreement with numerical calculations. The GAE activity can possibly induce enhanced fast particle losses. However, there is no experimental evidence for this effect in W7-AS. In particular, GAE's are absent at highest β , presumably due to broad profiles and low gradients in the core. Though the avoidance of rational surfaces inside

the plasma and the presence of a magnetic well, key elements for MHD stable stellarator plasmas, are not expected to prevent the GAE, it is difficult at present to predict GAE stability under reactor conditions. The stability will be determined by a subtle balance affected by electron and ion Landau damping, finite Larmor radius, and finite orbit width effects in the actual magnetic configuration. Specifically, the reduced average curvature (and therefore the reduced drive for kinetic mode excitation) in optimized stellarator configurations like the proposed W7-X could have a stabilizing influence on the GAE. Another beneficial effect could be caused by the relatively low velocities ($v_b \approx v_A/3$) of the energetic particles, which are resonant with the GAE. In particular in the case of thermalized α 's, it might turn out beneficial to enhance their losses.

It is a pleasure to acknowledge the assistance we have received from K. L. Wong, A. Boozer, B. Carreras, D. Sigmar, and K. Lackner.

-
- [1] C. T. Hsu and D. J. Sigmar, *Phys. Fluids B* **4**, 1492 (1992).
 - [2] D. J. Sigmar *et al.*, *Phys. Fluids B* **4**, 3695 (1992).
 - [3] K. L. Wong *et al.*, *Phys. Fluids B* **4**, 2122 (1992).
 - [4] K. L. Wong *et al.*, *Phys. Rev. Lett.* **66**, 1874 (1991).
 - [5] W. W. Heidbrink *et al.*, *Nucl. Fusion* **31**, 1635 (1991).
 - [6] A. D. Turnbull *et al.*, *Phys. Fluids B* **5**, 2546 (1993).
 - [7] C. Z. Cheng and M. S. Chance, *Phys. Fluids B* **29**, 3695 (1986).
 - [8] C. Z. Cheng, *Phys. Fluids B* **3**, 2463 (1991).
 - [9] G. Y. Fu and J. W. Van Dam, *Phys. Fluids B* **1**, 1949 (1989).
 - [10] S. Poedts *et al.*, *Plasma Phys. Controlled Fusion* **34**, 1397 (1992).
 - [11] L. Villard and G. Y. Fu, *Nucl. Fusion* **32**, 1695 (1992).
 - [12] M. S. Chu *et al.*, IAEA Würzburg Report No. CN-56/D-2-2, 1992.
 - [13] N. Nakajima *et al.*, *Phys. Fluids B* **4**, 1115 (1992).
 - [14] H. Ringler *et al.*, *Plasma Phys. Controlled Fusion* **32**, 933 (1990).
 - [15] K. Appert *et al.*, *Plasma Phys.* **24**, 1147 (1982).
 - [16] Yan Ming Li *et al.*, *Phys. Fluids* **30**, 1466 (1987).
 - [17] G. Y. Fu and J. W. Van Dam, *Phys. Fluids B* **1**, 2404 (1989).
 - [18] K. Appert *et al.*, *Phys. Fluids* **27**, 432 (1984).
 - [19] S. M. Mahajan and D. W. Ross, *Phys. Fluids* **26**, 2195 (1983).
 - [20] A. de Chambrier *et al.*, *Plasma Phys.* **24**, 893 (1982).
 - [21] T. E. Evans *et al.*, *Phys. Rev. Lett.* **53**, 1743 (1984).
 - [22] G. A. Collins *et al.*, *Phys. Fluids* **29**, 2260 (1986).
 - [23] We thank M. Ballico for providing the rf plasma production system.
 - [24] H. Biglari and L. Chen, *Phys. Rev. Lett.* **67**, 3681 (1991).
 - [25] N. N. Gorelenkov and S. E. Sharapov, *Phys. Scr.* **45**, 163 (1992).
 - [26] D. A. Spong *et al.*, *Phys. Fluids B* **4**, 3316 (1992).
 - [27] D. A. Spong *et al.*, *Bull. Am. Phys. Soc.* **37**, 1431 (1992).

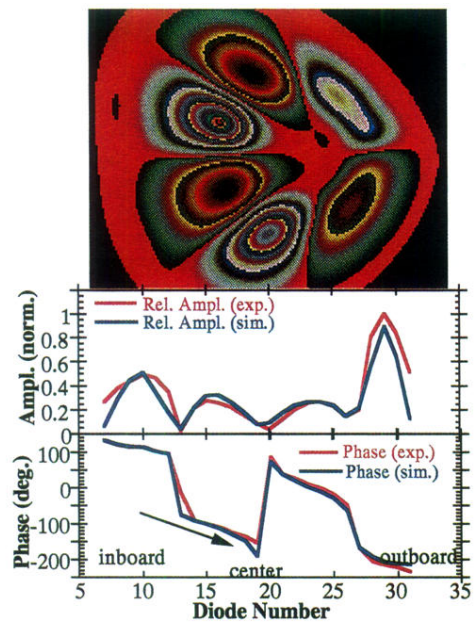


FIG. 3. The poloidal and radial mode structure ($m=3$ in this case) and the direction of propagation is determined from fitting the amplitudes and phases of the x-ray modulation by simulation calculations. On top the radial displacement distribution used in the simulation is given (-2.5 – $+2.5$ cm).

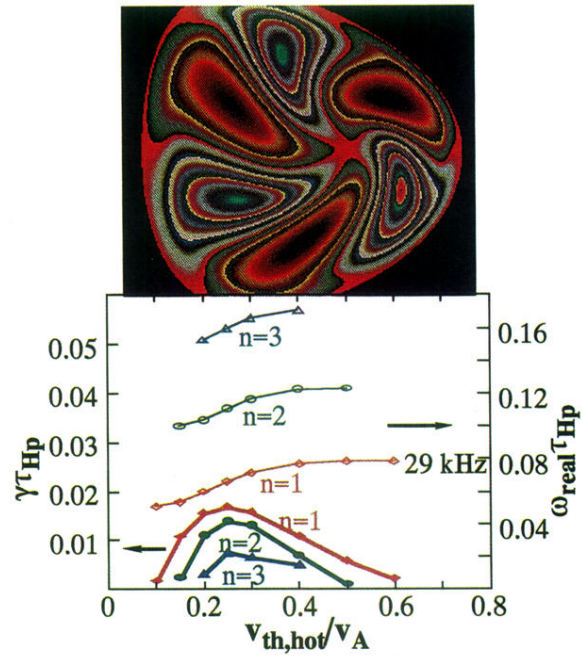


FIG. 5. $(m,n)=3,1$ mode structure from linear gyrofluid model calculation (top). Linear growth rates (including continuum and Landau damping) are highest for $n=1$ and peak around $v_b/v_A(0)=0.2-0.3$. Under the influence of the energetic particles the eigenfrequencies are shifted up (poloidal Alfvén time τ_{Hp}).